CHEMICAL ENGINEERING TRANSACTIONS
VOL. 81, 2020
A publication of AIDIC
The Italian Association of Chemical Engineering
Online at www.cetjournal.it
Guest Editors: Petar S. Varbanov, Qiuwang Wang, Min Zeng, Panos Seferlis, Ting Ma, Jiří J. Klemeš

ISBN 978-88-95608-79-2; **ISSN** 2283-9216
DOI: 10.3303/CET2081059

Multi-Physical Coupling Simulation of Thermal Effect on the Membrane Vibration Characteristics of Fabry-Perot Sensors

Shiwei Su[a], Wenrong Si[b], Chenzhao Fu[b], Pei Fu[a], Jian Yang[a,*], Qiuwang Wang[a]

[a]Key Laboratory of Thermo-Fluid Science and Engineering, MOE, School of Energy and Power Engineering, Xi'an Jiaotong University, Xi'an 710049, China
[b]State Grid Shanghai Electrical Power Research Institute, Shanghai 200437, PR China
yangjian81@mail.xjtu.edu.cn

Due to the anti-electromagnetic characteristics, high sensitivity and convenient installation, the Fabry-Perot sensor is commonly used in partial discharge detection of transformers. The variations of eigenfrequency and sensitivity caused by membrane temperature would have an important impact on sensor performance. In the present study, the eigenfrequency and displacement response of an intact membrane (IM) and a beam-supported membrane (BSM) under thermal expansion were numerically studied using a thin film vibration model coupled with temperature variations. The influence of the width and length for BSM's support beam on the stress softening was also analysed. It is found that the thermal expansion of the membrane reduces the stiffness and both the IM and BSM decrease linearly as temperature increases. The IM and BSM will become unstable as temperature increases to a certain value. The thermal stability of the BSM with support beam structure is lower than that of the IM. When the temperature increases, the IM amplitude increases and the BSM amplitude decreases. The eigenfrequency of the BSM is proportional to the width and inversely proportional to the length of the support beam, while the thermal stability is inversely proportional to the width and length of the support beam.

1. Introduction

People need a safer and more stable power supply system due to economic development. To meet people's production and living demand, the government has intensified the construction of smart grids and is committed to the integration of power grids and the Internet into one network (Huang et al., 2018). The transformer is the most critical and expensive equipment in the power system. To avoid the occurrence of insulation failure caused by partial discharge, on-line monitoring of the transformer is crucial. There are many methods to detect partial discharge, including chemical method, optical detection method, pulse current method, ultrasonic detection method and ultra high frequency method, etc (Pryor et al., 1994). Ultrasound has long been used in various detection fields. For example, Ma et al. (2017) had used the latest sound recognition localization algorithm and advanced wireless sensor network to monitor and study the status of safety valves in industrial production and achieved good results. Optical fibre sensors are widely used in partial discharge detection of the transformer because of their advantages such as anti-electromagnetic interference, high sensitivity, long-distance detection, small size and lightweight (Ma et al., 2013).
Deng et al. (2001) designed and tested a partial discharge detection system, which proved the feasibility of the application of F-P sensors in transformers. Ma et al. (2012) proposed a method for manufacturing sensors using thermal bonding. This method had a simple process and was easy to process, which allowed large-scale production of F-P membrane. Guo et al. (2012) provided a universal vacuum thermal vapour deposition method for membrane preparation and designed a sensor membrane with high sensitivity and high characteristic frequency by changing the diameter and thickness. In the above research, the feasibility of F-P sensors application, the material and manufacturing process of the membrane were studied, but the influence of the sensor working environment on the membrane was not considered and the important physical quantity of temperature was not introduced into the sensor application analysis. Wang et al. (2013) designed an F-P sensor with a tunable fibre laser, which can track the drift of the operating point when the ambient temperature

Paper Received: 18/03/2020; Revised: 28/05/2020; Accepted: 04/06/2020
Please cite this article as: Su S., Si W., Fu C., Fu P., Yang J., Wang Q., 2020, Multi-Physical Coupling Simulation of Thermal Effect on the Membrane Vibration Characteristics of Fabry-Perot Sensors, Chemical Engineering Transactions, 81, 349-354 DOI:10.3303/CET2081059

changes. The experimental result showed that the system could perform partial discharge detection well. Although the author considered the temperature change caused by the quadrature-phase point drift of the sensor membrane, it did not analyse the effect of the temperature field on the vibration characteristics of the membrane. Fu et al. (2017) proposed and analysed the beam-supported membrane (BSM) to solve the problem of low-temperature resistance of the intact membrane (IM) sensor. The result showed that the BSM structure had a good linear response region, but it did not analyse the effect of temperature on the BSM. Most of the researches on the design and test of the sensors are analysis of eigenfrequency and sensitivity under the consideration of constant temperature. However, there are few studies on the effect of temperature changes on the eigenfrequency and stability of the membrane. When the transformer works normally, the temperature inside the transformer will rise, which will cause the membrane thermal expansion, generate thermal stress and change the parameters. Changes in membrane vibration characteristics will cause the sensors to fail to accurately determine whether partial discharge has occurred.

In this paper, the vibration model of the membrane coupled with the temperature field, is established to analyse the vibration characteristics of the membrane when the temperature changes. The thermal expansion, stress softening and parameter changes of the membrane are analysed by the membrane vibration mode. The thermal effect of the BSM is also analysed. The relationship between the eigenfrequency and temperature of the IM and the BSM is obtained. The length and width of the BSM's support beam structure have a great influence on the parameters of the membrane. The eigenfrequency analysis and thermal stability analysis of the length and width of the beam are also performed in this paper. The effect of temperature on the membrane was studied and the relationship between the geometric parameters of the beam support structure and the eigenfrequency, amplitude and thermal stability were discussed, which will help to optimize the design of the sensor in the future.

2. Method and Simulation

2.1 Method

The working principle of F-P sensors is shown in Figure 1. The sensors consist of optical fibre, resonant cavity and membrane. In the transformer, the partial discharge generates ultrasonic waves, which will cause the membrane to vibrate and affect the length of the resonant cavity L. The formula of the relationship between the intensity of the reflected light and the length of the resonant cavity is shown by Eq(1), where L represents the length of the resonant cavity, λ represents the wavelength of light, R_1 and R_2 represent the reflectance of the two end faces, and I_0 represents the intensity of light source (Si et al., 2017).

$$I_r = I_0 \frac{R_1 + R_2 - 2\sqrt{R_1 R_2}\cos(\frac{4\pi L}{\lambda})}{1 + R_1 R_2 - 2\sqrt{R_1 R_2}\cos(\frac{4\pi L}{\lambda})} \tag{1}$$

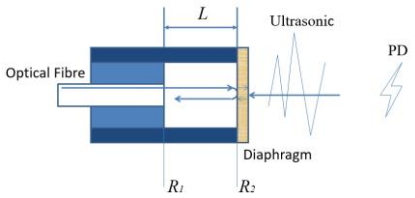

Figure 1: Schematic diagram of Fabry-Perot sensor

At present, the F-P sensors use a complete circular membrane (IM) with a fixed boundary. The IM sensors resonant cavity is not connected to the environment. When the internal and external pressures are different, the operating point of the sensors will drift and affect the normal operation of the sensors. In order to improve the signal-to-noise ratio of the sensors, Fu et al. (2017) proposed a BSM structure membrane. Because the internal and external media of the BSM structure are connected, the internal and external pressures of the membrane can be controlled to be equal.

The circular membrane of the sensor vibrates freely in the transverse direction. The differential equation of motion is shown by Eq(2).

$$EI\frac{\partial^4 w(r,\theta,t)}{\partial x^4} + \rho A\frac{\partial^2 w(r,\theta,t)}{\partial t^2} = 0 \tag{2}$$

Where w represents the displacement of the membrane; E represents Young's modulus; I represents the moment of inertia of the section; A represents the cross-sectional area of the beam (Decuzzi et al., 2007).
The boundary conditions are shown by Eq(3).

$$w(R,\theta,t)=0\,,\ \frac{\partial w}{\partial x}(R,\theta,t)=0 \tag{3}$$

Where R is the radius of the membrane. The thermal stress caused by the thermal expansion of the membrane is shown by Eq(4).

$$\sigma_{\mathrm{t}}=\frac{E}{1-\mu^{2}}\cdot\alpha\cdot\Delta T \tag{4}$$

Where μ is the Poisson's ratio, α is the thermal expansion coefficient and ΔT is the temperature difference.
In this study, the finite element software COMSOL Multiphysics was used to solve the eigenfrequency and stress softening of IM and BSM at different temperature. The length and the width of the cantilever structure of BSM were quantitatively calculated.

2.2 Simulation

The simulated physical models are shown in Figure 2. Figure 2a represents the structure of IM and the periphery of IM is a fixed constraint boundary condition. Figure 2b shows the BSM structure, which is composed of a circular membrane and four cantilever beams and the ends of the beams are fixed boundaries. The membranes are made of quartz. The thickness of the membranes is 40 μm and the diameter of the central circular membranes are 1.2 mm. The solid mechanical physics field is used to solve the eigenfrequency of the membrane.

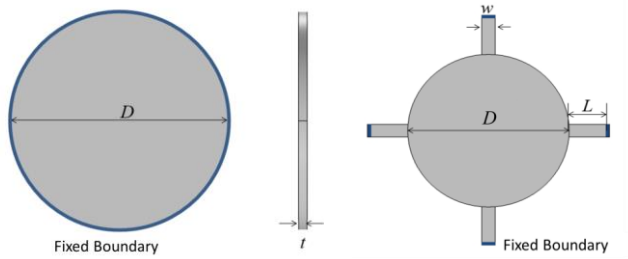

(a) (b)

Figure 2: Geometric model of (a) IM and (b) BSM structure

In analysing the relationship between the natural frequency and the temperature of the IM and BSM structures, the natural frequency when the temperature increases by 10 K, 20 K, 30 K, 40 K, 50 K, 60 K, 70 K, 100 K, 200 K and 300 K are solved. When analysing the influence of the width w of the BSM cantilever structure on the membrane parameters, based on the length of 0.3 mm, the width was selected as 0.05 mm, 0.08 mm, 0.1 mm, 0.12 mm, 0.15 mm, 0.18 mm, 0.2 mm, 0.25 mm and 0.3 mm for calculation. In analysing the influence of the length L of the BSM cantilever structure on the parameters of the membrane, the width was selected as the basis of 0.1 mm, and the length was selected from 1.5 mm, 1.8 mm, 2 mm, 2.2 mm, 2.5 mm, 3 mm, 4 mm, 5 mm and 6 mm for calculation. The physical properties of the material are shown in Table 1.

Table1: Physical properties of the membrane

Name	Density ρ	Young's modulus E	Poisson's ratio v	Thermal expansion coefficient α
Membrane	2,201 (kg/m^3)	80 (GPa)	0.17	0.00001 (1/K)

The theoretical solution for the first-order eigenfrequency of the free vibration of a fixed circular membrane is shown by Eq(5).

$$f=\frac{10.21t}{2\pi r^{2}}\sqrt{\frac{E}{12r(1-\nu^{2})}} \tag{5}$$

In the formula, t represents the thickness and r is the radius of the membrane. The theoretical solution for the IM is 318.22 kHz and the finite element method is 315.70 kHz with an error of 0.79 %. The feasibility of using the finite element method is verified.

3. Results and Discussion

3.1 Effect of Temperature on Eigenfrequency

The relationship between the natural frequency and temperature of IM and BSM are shown in Figure 3.

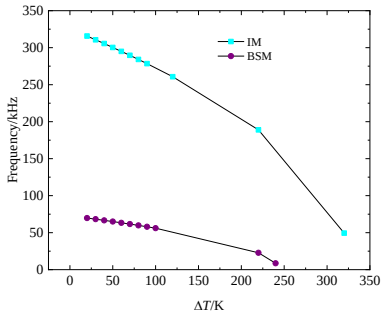

Figure 3: Relationship between eigenfrequency and temperature

(a) (b)

Figure 4: Mode shapes (a) IM and (b) BSM structure

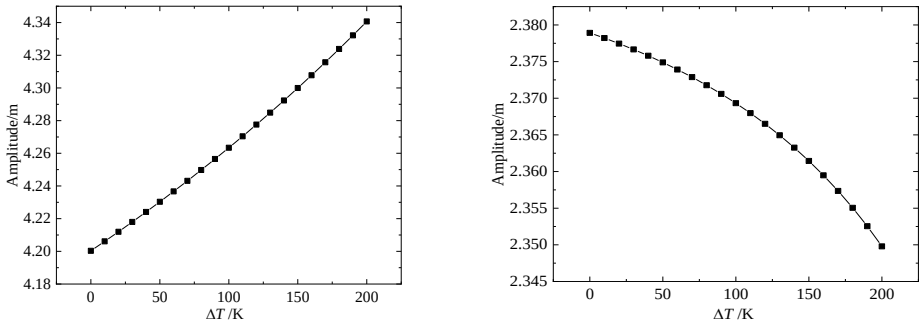

(a) (b)

Figure 5: Amplitude vs. temperature curve (a) IM and (b) BSM structure

It can be observed that both the vibration mode of IM and BSM show a strong temperature dependence, their natural frequencies decrease as the temperature rises. The IM are more affected by temperature than the BSM. When the temperature rise is lower than 220 K, the natural frequency decreases linearly, for every 10 K increase in temperature, the natural frequency of the IM decreases by 5 kHz and the BSM decreases by 1.5 kHz. When the temperature rises to 220 K, the natural frequency will decrease rapidly. For every 10 K increase in temperature, the natural frequency of the IM decreases by 14 kHz and the BSM decreases by 7.1 kHz. For the boundary conditions of fixed constraints, compressive stress will be generated when the membrane is thermally expanded, causing the stiffness of the membrane to decrease. It can be seen from the mode diagram of Figure 4 that the boundary of the IM is fixed constraints and the displacement of the membrane from the boundary to the centre gradually increases. Due to the BSM has fixed constraints at the cantilever structure and the rest of the membrane unconstrained, the BSM only has a large displacement at the cantilever when it vibrates and the central membrane vibrates as a whole, so when the temperature increases, the impact on the BSM stiffness is less than the impact on the IM.

3.2 Sensitivity

The relationship between the amplitude and the temperature of IM and BSM when resonance occurs is shown in Figure 5.
As the temperature increases, the amplitude of the IM gradually increases, while the amplitude of the BSM gradually decreases. For the IM, the annular boundary is a fixed constraint and the membrane stress is softened due to temperature rise, so the amplitude will increase when resonance occurs. But for the BSM, because most of the membrane is a free boundary, only the cantilever part is fixed and the thermal expansion of the round membrane part will affect the cantilever beam, causing the amplitude of the BSM to decrease with increasing temperature.

3.3 Influence of Cantilever Structure Parameters on BSM

The natural frequency and stress softening of the BSM with cantilever structures of different lengths are solved. The results are shown in Figure 6a.

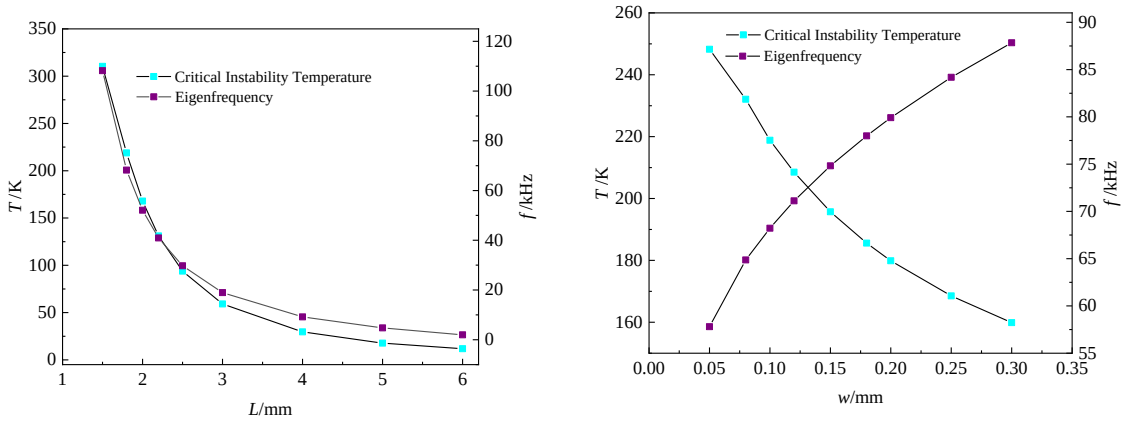

Figure 6: The effects of the beam length (a) and the beam width (b) on BSM

With the increase of the length of the cantilever beam, the natural frequency decreases and the decreasing speed gradually becomes slower. The critical load temperature of the membrane also gradually decreases and the decreasing trend is similar to the eigenfrequency. When the length of the cantilever is increased, the entire structure is closer to the cantilever beam model fixed at both ends. When the temperature increases, the increase in the length of the cantilever beam will cause the volume change of the membrane to increase, the stress of the membrane to increase, the rigidity to decrease and the critical thermal load to decrease.
The solution results for the BSM with different widths are shown in Figure 6b. The natural frequency increases gradually as the width of the cantilever structure increases. The increase of the width of the cantilever structure leads to an increase in the fixed constraint boundary of the membrane and the natural frequency of the membrane moves to the direction of the fixed boundary of the membrane as a whole. The critical temperature load of the membrane decreases with increasing width. As the width increases, the free border of the membrane decreases. For the BSM, the increase in temperature mainly affects the stress on the membrane by affecting the cantilever structure and the increase in width means that the stress increases, reducing the thermal stability of the membrane.

4. Conclusions

In this paper, the FEM is used to solve the vibration characteristics and thermal stability of IM and BSM. The effects of the length and width of the cantilever support structure on the BSM are analysed. The specific results are as follows:
1) An increase in temperature will cause the eigenfrequency of IM and BSM to decrease. When the temperature difference is low, the eigenfrequency is linearly related to the temperature change. When the temperature increases to a certain temperature, the eigenfrequency decreases rapidly.
2) The temperature change will affect the stiffness of the membrane, so the amplitude at resonance will be affected. As the temperature increases, the amplitude of the IM at the natural frequency increases too. The amplitude of the BSM at the natural frequency decreases with increasing temperature.

3) For the BSM, the increase of the length of the cantilever structure will reduce the eigenfrequency and the thermal stability; increasing the width will increase the eigenfrequency and decrease the thermal stability.

Acknowledgements

This work was supported by the S&T project of State Grid Corporation of China: “Research and application of key technologies of integrated ultrasonic and UHF PD coupling and sensing in transformer” under grant number of 52094019000S.

References

Decuzzi P., Granaldi A., Pascazio G., 2007, Dynamic response of microcantilever-based sensors in a fluidic chamber, Journal of Applied Physics, 101, 024303.

Deng J.D., Xiao H., Huo W., Luo M., May R., Wang A.B., Liu Y.L., 2001, Optical fiber sensor-based detection of partial discharges in power transformers, Optics and Laser Technology, 33, 305-311.

Fu C.Z., Si W.R., Li H.Y., Li D.L., Yuan P., Yu Y.T., 2017, A novel high-performance beam-supported membrane structure with enhanced design flexibility for partial discharge detection, Sensors, 17, 593-604.

Guo F.W., Fink T., Han M., Koester L., Turner J., Huang J.S., 2012, High-sensitivity, high-frequency extrinsic Fabry-Perot interferometric fiber-tip sensor based on a thin silver membrane, Optics Letters, 37, 1505-1507.

Huang Y.M., Hu C.Q., You Z.S., 2018, Analysis for chemical thermal reaction of optical fibre composite low-cable based on finite element analysis, Chemical Engineering Transactions, 71, 469-474.

Ma J., Jin W., Ho H.L., Dai J.Y., 2012, High-sensitivity fiber-tip pressure sensor with graphene membrane, Optics Letters, 37, 2493-2495.

Ma J., Xuan H.F., Ho H.L., Jin W., Yang Y.H., Fan S.C., 2013, Fiber-optic Fabry-Pérot acoustic sensor with multilayer graphene membrane, IEEE Photonics Technology Letters, 25, 932-935.

Ma J.Z., Lu J.Q., 2017, Application of wireless sensor based on sound localization in safety valve condition monitoring of chemical plant, Chemical Engineering Transactions, 62, 745-750.

Pryor B., 1994, A review of partial discharge monitoring in gas insulated substations, IEEE Colloquium on Partial Discharges in Gas Insulated Substation, 1, 1-2.

Si W.R., Li H.Y., Fu C.Z., Yuan P., Yu Y.T., 2017, Essential role of residual stress in fiber optic extrinsic Fabry-Perot sensors for detecting the acoustic signals of partial discharges, Optoelectronics and Advanced Materials-Rapid Communications, 11, 637-642.

Wang Q.Y., Ma Z.H., 2013, Feedback-stabilized interrogation technique for optical Fabry-Perot acoustic sensor using a tunable fiber laser, Optics and Laser Technology, 51, 43-46.